Creep properties of 1.25Cr-1Mo-0.25V steels for turbine casings

Sergio G. Hernández

Monterrey Forgings, Monterrey N.L. México
Instituto Tecnológico de Morelia, Metallurgy department
Av. Tecnológico 1500. Col. Lomas de Santiaguito 58120 Morelia, México
E-mail: shernandez@forja-mty.com.mx

Alberto N. Conejo

Professor
Instituto Tecnológico de Morelia, Metallurgy department
Av. Tecnológico 1500. Col. Lomas de Santiaguito 58120 Morelia, México
E-mail: aconejo@itmorelia.edu.mx

Resumen

El acero resistente al calor, 1.25Cr-1Mo-0.25V, empleado en la fabricación de carcazas de alta presión para turbinas de vapor, fue sometido a ciclos de tratamiento térmico que involucran recocido, temple y revenido, con el objeto de obtener elevadas propiedades mecánicas, en particular resistencia a la ruptura a altas temperaturas. Se empleo el parámetro Larson-Miller para predecir resultados de tiempos de prueba muy largos (3000-20000 horas) a partir de someter las piezas a tiempos de prueba mucho mas cortos (50 horas). Las predicciones obtenidas indican tiempos de ruptura mayores que los experimentales, sin embargo, la metodología propuesta puede ser de utilidad con objeto de obtener una estimación rápida y así realizar acciones correctivas durante el proceso de manufactura.

Palavras-chave: Termofluencia, Parámetro Larson-Miller, carcazas.

Abstract

A heat resistant steel, 1.25Cr-1Mo-0.25V, produced by a casting process and used in the manufacture of turbine casings, has been heat treated with a combination of thermal cycles that involve annealing, quenching and tempering in order to obtain high mechanical properties - in particular, rupture-strength at high temperatures. The Larson-Miller Parameter has been used to predict results from short-time tests (50 hours) with those obtained at longer times (3000-20000 hours). The predictions resulted in higher rupture-times. However, the current methodology can provide a rapid estimation of creep-behavior at longer times from short-time tests in order to take corrective actions during the manufacturing process.

Keywords: *Creep, creep-rupture time, creep-rupture strength, Larson-Miller parameter.*

1. Introduction

Electricity generation capacity in Mexico reached 39,350 MW. in 2001. By the year 2007, additional requirements of 21,000 MW are estimated (http// www.fe.doe) in order to cope with the growing demand. Most of the power plants in México are fossil steam power plants whose share is close to 50% of the current generation capacity. According to the current energy policy, a conversion of several thermoelectric plants to natural gas by the year 2005 is expected. This scenario involves the construction of additional power plants in the near future.

Operational conditions in a power plant involve high pressures and high temperatures. In order to improve thermal efficiency of power plants, heat transfer losses must be reduced to a minimum. This is accomplished by raising the steam's pressure and temperature. Historical development of fossil-fired turbine-generators (Masuyama, 2001) indicates that due to the use of carbon steel as a construction material by the 1920´s, the maximum limits on steam pressure and temperature were 4 MPa and 370ºC, respectively. When Mo was added to the steel, the operational conditions were raised to 10 MPa and 480ºC. In the 1940´s, the use of Cr-Mo steels allowed operational conditions of 17 MPa and 566ºC. This race continued up to the 1960´s when power plants operating up to 34 MPa and 650ºC were built. However production costs abruptly increased, motivating a return to operational conditions, in most plants, to 24 MPa and 538ºC. A cyclic shortage of oil will lead to increases in steam pressure and temperature in order to reduce thermal losses.

The main components of a fossil fuel power plant are rotors and casings. The types of steels for these components are divided into two major groups; Ferritic and austenitic steels. Ferritic steels have the advantage of lower cost and higher thermal stability due to a low thermal expansion coefficient, a feature suitable for plants undergoing frequent start and stop cycles according to changes in electricity demand. Cr, Mo, V, Si and Al increase the temperature range over which ferrite is stable, meanwhile Ni, Mn, C and N stabilize austenite. Cr is a basic element used to provide oxidation and corrosion resistance. Mo and W increase solution strengthening. V and Ti combine with C and/or N to produce carbides, nitrides or carbonitrides.

Creep strength is the most important mechanical property for high pressure and high temperature applications. Creep strength has been increased to withstand stresses up to 140 MPa at 600ºC in modern heat resistant steels. Creep is defined as the time-dependent strain that occurs after the application of a load which is thereafter maintained constant. When carbon content increases above 0.1% reduce creep strength, its maximum concentration is bound to an upper limit. There is also experimental evidence that when the Mo equivalent (Mo + 0.5W) is set at 1.5%, higher creep strength is obtained. For turbine components operating up to 566ºC, Cr-Mo-V steels are commonly employed.

Casing is a turbine component that serves to enclose rotor-generators (low pressure and intermediate-high pressure). Because of its complex geometry and large variation in wall thickness, casings are produced by sand casting processes. The manufacturing process requires deep knowledge both in the production of clean steels and in the solidification behavior during casting. Because of the large variation in wall thickness the casing is subjected to different cooling speeds which cause residual stresses. This issue is taken into account both during casting and heat treatment.

A casing is designed on the basis of long-term creep-rupture strength and fracture toughness. Creep properties are defined in terms of a minimum creep-rupture time, however, usually such period of time is very long, in the order of 10^3-10^6 hours. The objective of this work is on one side to define the heat treatment process which will result in high mechanical properties, and the other, to assess the use of the Larson Miller Parameter, P(σ), to drastically reduce the time of the creep test and subsequently extrapolate these results to predict long-time rupture-tests.

2. Experimental work

The steel was produced in an AC-Electric Arc Furnace with a nominal capacity of 45 tons. Together with the casting process of the casing, five trial pieces were casted separately. This material was employed for evaluations in the present work. Figure 1 shows the dimensions of such pieces. After casting, the trial pieces were annealed, followed by the removal of feeders and risers. Before a preliminary rough-machining, they were heat treated to relief stresses and after that a set of planned heat treatments were carried out in order to define conditions to produce the mechanical properties specified by the customer. Specimens for tension, impact and creep tests were specially machined in accordance with ASTM and DIN standards.

The casing produced is a split-type. It operates in the high-pressure section of a steam turbine designed to produce 350 MW of electrical energy.

Chemical analysis was done with an optical emission spectrometer, Bausch and Lomb model 3560 AES, with a capacity to detect 23 elements. Carbon and sulphur were measured with a LECO apparatus, model CS-244. Heat treatments were conducted with the aid of a furnace manufactured by Honeywell, with capabilities to heat from 600-1000°C (temperature was recorded with the aid of an R-type thermocouple) and the furnace had a heating rate capacity up to 300 C/hr. To conduct the tension test, a universal tension machine was used. The machine was a Tinius Olsen , model super L with a capacity of 60 tons, equipped with a furnace to conduct tests up to 1093°C at a maximum heating rate of 500 C/hr. The impact test was

conducted with a Tinius Olsen machine with a capacity of up to 36.5 kg-m (358 Joules) and a vertical height of 1.34 m. In this machine Charpy specimens (CVN) were employed. To define the transition-temperature ductile-fragile (FATT), a liquid bath capable to cool the specimen up to –150°C was used. To conduct the hardness test, a Wilson machine to measure Brinell hardness (BHN) and a Future-tech machine to measure Vickers hardness (VHN) were employed. Microstructural analysis were carried out with the aid of a Leitz Wetzlar optical microscope, model MM6.

The equipment employed to carry out the short-time creep-rupture tests was a SATEC machine, model M-3, with a total capacity of 3000 kgs, maximum testing temperature of 1200°C and a lever arm ratio of 16:1. All creep testing followed the procedures established in ASTM E139 (ASTM,1996). Testing was conducted under constant load. Strain measurements are made using tube extensometers clamped to the specimen shoulders. Temperature control of the furnace is achieved by the use of a thermostat which controls the on-off power to the furnace. K-type thermocouples were attached to each specimen. Prior to testing, several measurements are made in order to define the load applied.

To set up the creep test the furnace is packed with insulating material for efficient temperature control. The specimen is heated to the specified temperature allowing a minimum of 1 hr for the temperature to stabilize. The final test load is achieved by applying weights in calculated increments. Once the full load is applied, the test hours are recorded until rupture occurs.

In order to avoid energy shutdowns, special back up is required. Long-time rupture-tests were conducted at external laboratories (MCL labs, USA).

The results were analyzed based on the empirical relationship to predict rupture-stress developed by Larson and Miller (Larson and Miller, 1952). This relationship is commonly employed in industrial practice. The Larson-Miller Parameter, P(σ), is given by the following relationship (ASM, 1978; Riedel, 1986):

$$P(\sigma) = \frac{\Delta H}{R} = T\,(C + \log t) \times 10^{-3} \qquad (1)$$

Where:

T = Absolute temperature in °K.

C = Constant.

t = time for rupture in hours.

The constant C can be obtained from a plot log t_r versus the reciprocal of temperature, fixing the initial stress. The amount of data generated in this work was not enough to compute a reliable value for C, therefore, taking into consideration that for most low alloy steels the magnitude of this constant is approximately 20, such value was used in the present computations.

3. Results and discussion

The chemical composition of the steel produced is shown in Table 1. The low levels of residual elements can be noted. This is important to avoid temper embrittlement. Watanabe (in Grosse et.

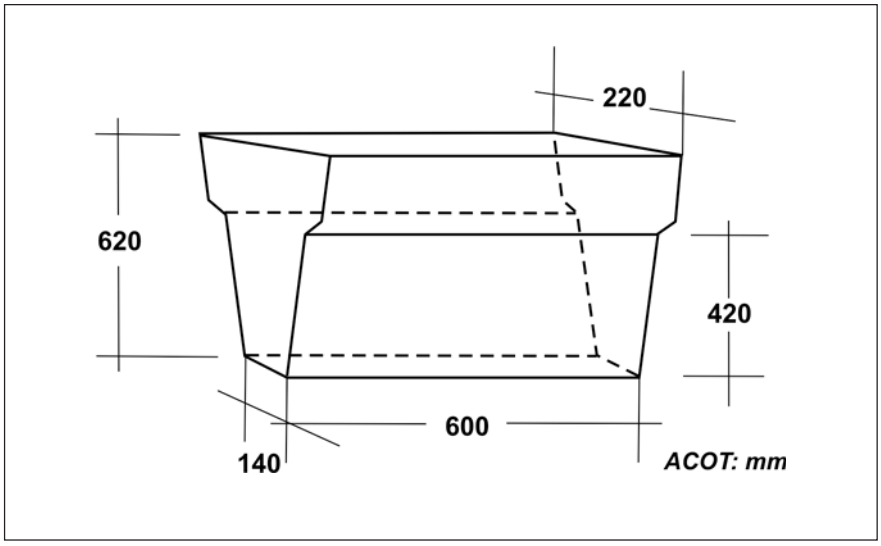

Figure 1 - Dimensions of trial pieces.

Table 1 - Chemical steel composition of experimental heat, wt %.

		C	Si	Mn	P	S	Cr	Mo	V	Al	Ni	Cu	Sn	As	Sb
Heat		0.16	0.32	0.68	0.007	0.004	1.27	1.03	0.26	0.004	0.05	0.04	0.004	0.002	0.0008
Final Product		0.16	0.30	0.66	0.004	0.003	1.25	1.05	0.26	0.003	0.05	0.04	0.002	0.002	0.0008
Specs	**Min**	0.15	0.30	0.50	--	--	1.00	0.90	0.20	--	--	--	--	--	--
	max	0.20	0.50	0.80	0.030	0.030	1.50	1.15	0.30	0.030	--	--	--	--	--

al., 1982) formulated the following factor related to temper embrittlement:

$$J = (Mn + Si) \cdot [(P + Sn) \times 10^4] \quad (3)$$

To reduce the potential for temper embrittlement, this factor should be lower than 120. The J factor for the steel produced is less than 60. Antimony and Arsenic also have a tremendous influence on temper embrittlement. This influence is taken into account in the following coefficient for temper embrittlement:

$$F = (2Si + Mn \text{ in wt\%}) \cdot (10P + 5Sb + 4Sn + As, \text{ in ppm}/100) \quad (4)$$

When this factor increases, FATT also increases.

At high temperatures the grain boundary has lower strength than the grain; such behavior promotes intergranular fracture. Aluminum is a grain refiner. However, it is usually avoided in heat resistant steels because it shows a high tendency to precipitate on the grain boundaries as AlN, thus, decreasing their strength, in contrast to other grain refiners such as titanium which precipitate in a more homogeneous manner.

The final concentration of carbon reported in the product was 0.16%. This level is in agreement with the maximum limit identified (Buchi and Sidey, 1965) on the limit to suppress the formation of cementite in 1%Cr-Mo-V steels. Cementite has a deleterious effect on creep strength. In this type of steels vanadium carbides are desired to reduce the movement of dislocations.

Annealing and oil quenching temperatures were fixed at 920 and 960°C, respectively. This temperature falls within the austenitic zone. More details of the heat treatments can be seen in Figure 2. Transformation temperatures, Ac_1 and Ac_3, were analyzed taking into consideration the correlations reported by Cias (Cias, 1977) as well as the Atlas of CCT diagrams (ASM, 1977). With this information Ac_1 and Ac_3 were estimated, yielding 745°C and 880°C, respectively, as well as the critical cooling speed to obtain baintite after quenching at 8 C/min. An actual cooling rate of about 5-15 times faster than that determined from CCT curves is suggested in order to control the size and distribution of precipitated particles throughout the matrix.

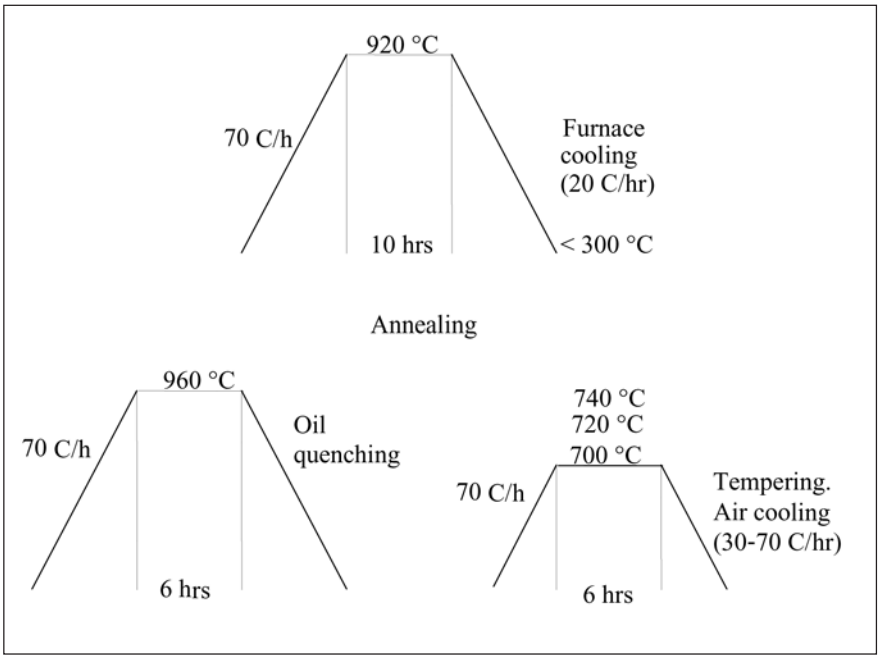

Figure 2 - Heat treatments for turbine casing.

Actual measurements on the trial pieces during oil quenching resulted in a cooling speed of 100 C/min.

The final tempering temperature was selected based on the development of a master curve for tempering. Such a curve requires plotting the results of mechanical properties as a function of $P(\sigma)$. Three temperatures were analyzed as a first approximation, 700, 720 and 740°C, with a holding temperature of 6 hours. Table 2 and Figure 3 show the results of mechanical properties after quenching and tempering at three temperatures as well as the master curve displaying such results as a function of $P(\sigma)$. Table 2 also shows the minimum values in mechanical properties specified by the customer. The chemical composition and mechanical properties for turbine casings were reviewed by Kobayashi (Kobayashi et. al., 1977). The values provided in this table correspond to typical values of such components. In Figure 3, it can be seen that a $P(\sigma)$ of 20.84 and its corresponding tempering temperature of 730°C, yield mechanical properties which fall in the middle of the specifications for tensile strength. Furthermore, the other mechanical properties are above the minimum requirements. Figure 4 shows in more detail the results on impact properties to evaluate FATT. As the tempering temperature is increased from 700 to 740°C, the transition-temperature decreased from 20°C to –2°C. FATT at 730°C was reported to be 5°C.

Evaluation for creep properties at high temperatures and constant load was conducted for materials in the condition of annealing, quenching and final tempering at 730°C. The customer specifies the minimum requirements of time before rupture occurs at a given set of conditions of stress and temperature. The minimum creep-rupture times at a given set of conditions of temperature and applied stress (nominal values) are indicated in Table 3. Minimum creep-rupture times range from 1000 to 8000 hours for a temperature range from 550 to 600°C and applied stresses ranging from 90 to 200 MPa. Because of such

long times, it would be desirable to have an additional tool to estimate "long-time" creep properties from "short-time" tests. By using P(σ), it is possible to achieve this goal, trading off time for temperature. This means that if the time is reduced, then, the temperature should be increased. The new testing temperature for short-time tests is determined based on the nominal Larson-Miller parameter computed for long-time rupture-tests and the time for the "short-time" test which was set arbitrarily at 50 hours. The nominal P(σ) is thus computed using the minimum requirements of stress-rupture time and the nominal temperature. For example, a creep test conducted under a stress of 200 MPa and 550°C must resist at least 1000 hours before rupture occurs. With this data, the magnitude of the nominal P(σ) is equal to 18.93. This value is fixed as a constant to compute the new testing temperature by substituting the nominal P(σ) and the new time for the short-time test (50 hours), which yields 599°C.The new temperatures for the "short-time" tests are also shown in Table 3. Thus, "short-time" creep tests are now associated with a "higher-temperature" range, as compared with the "long-time" creep tests associated with a "lower-temperature" region. With this procedure, the increment in temperature changed from 49 to 84°C over the nominal temperature range.

Reliable results can be extrapolated to longer times only when it is certain that no structural changes occur in the region of extrapolation which would produce a change in the slope of the curve (Dieter,

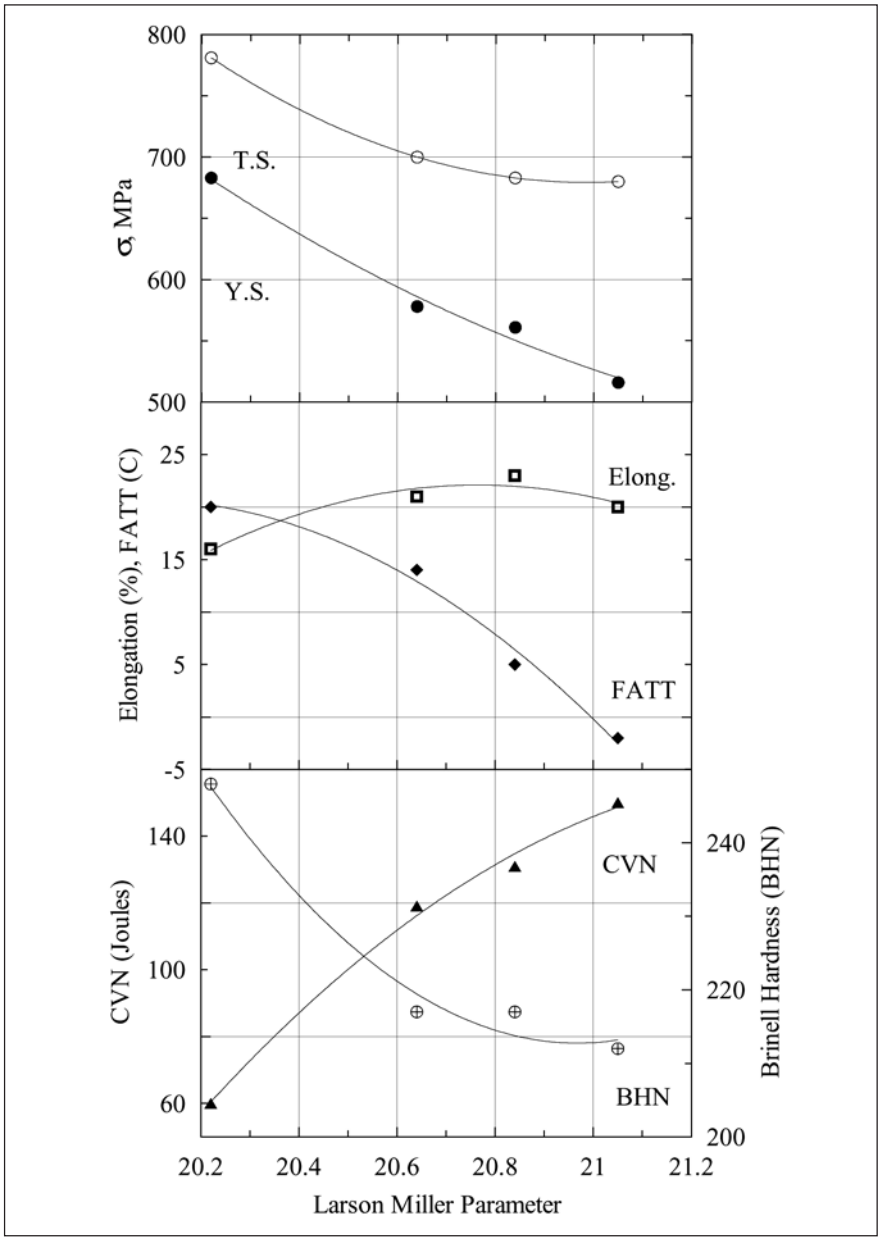

Figure 3 - Master curve indicating the mechanical properties after tempering at different temperatures as a function of the LMP.

Table 2 - Results of mechanical properties as a function of tempering tempeature.

Tempering Temperature, °C		TS, MPa	YS, MPa	El, %	ratio TS/El	BHN	U_T, avg, Joules	FATT, °C	LMP
700		781	683	16	12500	248	60	20	20.22
720		700	578	21	14700	217	119	14	20.64
740		680	516	20	13600	212	150	-2	21.05
Specs	**min**	590	440	15	10500	170	24	--	
	max	780	--	--	--	225	--	--	

1976). The results obtained with "short-time" tests will be extrapolated at longer times and then compared with current results determined in "long-time" tests.

Figure 5 displays the continuous deformation experienced with time as a function of temperature and initial stress for the "long-time" tests. From this information, the design stress can be selected so that the total creep deformation does not exceed a certain value in the lifetime of the part for the particular temperature used. The typical stages in a creep test can be more clearly visualized plotting creep rate versus time. This is shown in Figure 6. Secondary creep is represented by the segment with a constant creep rate. Fracture occurs in the last portion of the test, also known as ternary creep. It can be observed that the creep-rupture time increases by decreasing both the initial stress and temperature.

Table 4 shows the results for the actual rupture-times and the corresponding values for P(σ), for both, short-time and long-time tests. It can be noticed that for all cases, the actual results for the creep-rupture time are much longer than the nominal times. This, in principle, is a first indication of high creep rupture strength and evidence of a good manufacturing process.

A typical master curve using P(σ) involves a logarithmic scale for the applied stress. The results are displayed in Figure 7. This plot correlates, simultaneously, the stress-rupture time, temperature and applied stress. Consequently a relationship between P(σ) and the applied stress can be employed as a basis to compute the rupture-time for long time tests. The following equation fits the results for "short-time" tests:

$$(\sigma) = 1408 - 62.3 \cdot P(\sigma) \qquad (4)$$

With this equation, the value of P(σ) can be re-calculated for a given initial stress. The new values are then employed to predict creep-rupture times substituting the "low-temperature" corresponding to "long-time" creep tests. For example, the "long-time"

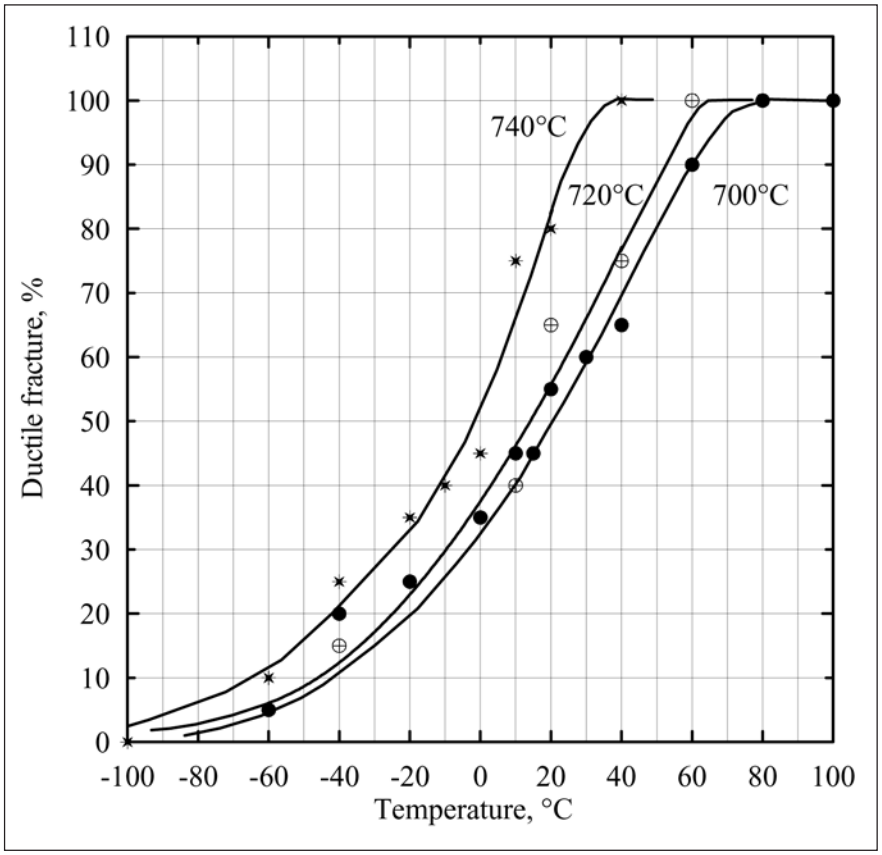

Figure 4 - Fracture Appearance Transition-Temperature Test (FATT).

Table 3 - Minimum requirements for the creep-rupture tests.

Long-time rupture tests				Short-time rupture tests		
T, °C	σ, Mpa	t_{min}, hr	LMP_{specs}	t_{min}, hr	T, °C	σ, Mpa
550	200	1000	18.93	50	599	200
550	175	3000	19.33	50	617	175
550	150	8000	19.68	50	634	150
575	**150**	**1000**	**19.51**	**50**	**626**	**150**
575	**135**	**3000**	**19.91**	**50**	**645**	**135**
575	**120**	**6000**	**20.17**	**50**	**656**	**120**
600	120	1000	20.08	50	652	120
600	100	4000	20.61	50	677	100
600	90	6000	20.76	50	684	90

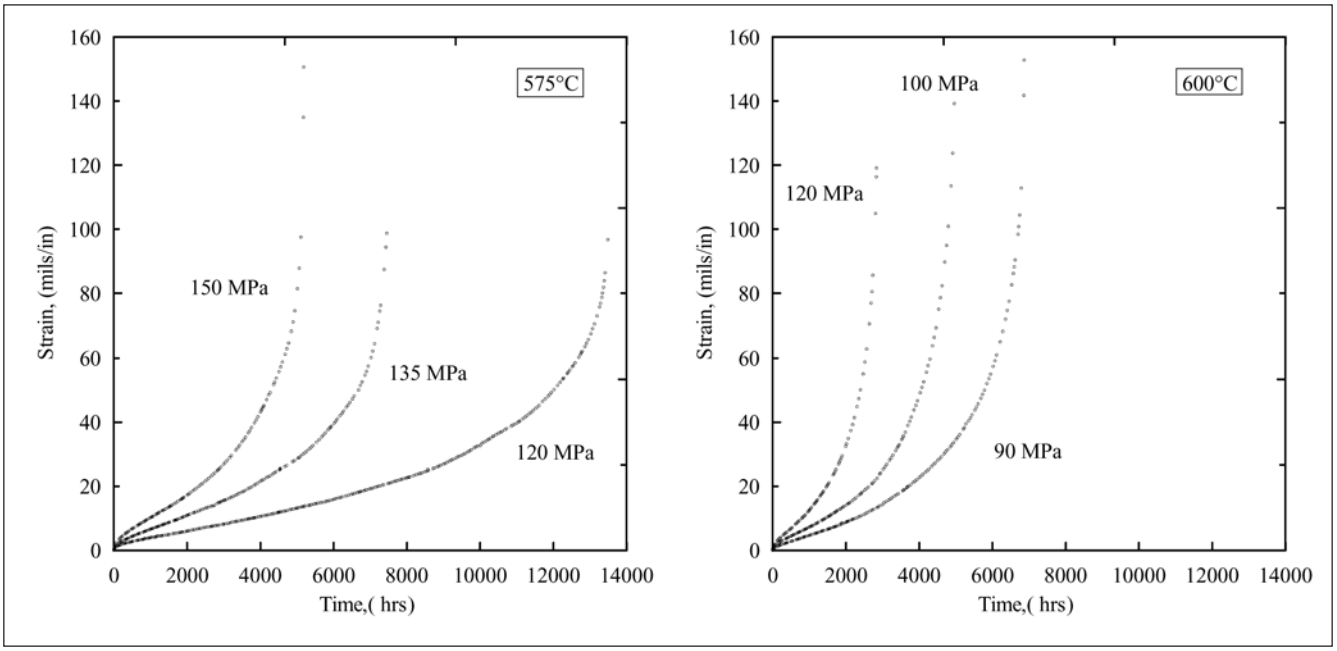

Figure 5 - Creep curves under constant load at two temperatures.

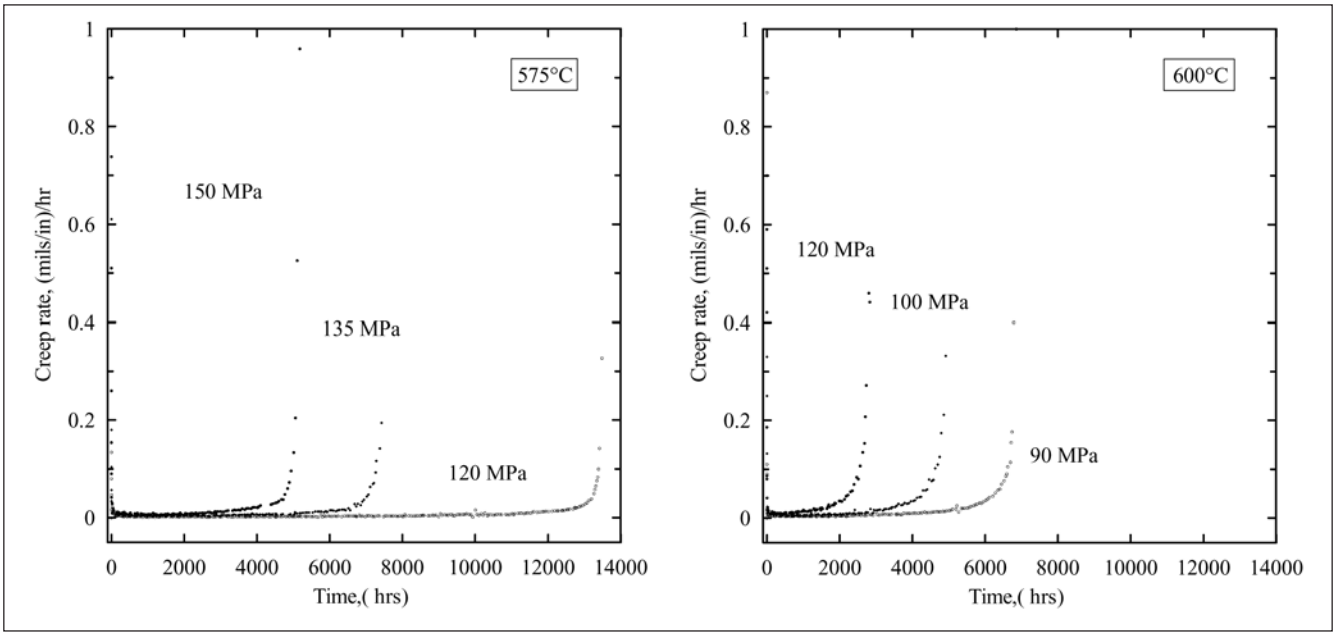

Figure 6 - Creep-rate curves at two temperatures and as a function of the initial stress.

rupture-test with an initial stress of 200 Mpa and 500°C must be conducted for at least 1000 hours (41 days) without failure in order to comply with the specifications. In accordance with the present methodology, the "short-time" test was conducted for 50 hours but at 599°C. Under these conditions, the rupture-life was 178 hours when the experimental $P(\sigma)$ value is 19.38. This value is then replaced in Equation (1) to predict the rupture-life at any other temperature with the same initial stress. For 550°C, the predicted rupture-life is 3497 hours. The experimental value for the long-time test gave a similar value of 3521 hours.

Comparing the results for both cases, as shown in Figure 7, a larger slope for the results obtained during creep tests at short-times is observed. It can also be seen that as the rupture-life increases the error in the prediction also increases. As the deviation in both slopes increases, the disagreement between real rupture-time and predicted values increases.

Another comparison of results using real and predicted rupture-times (equation 4) is shown in Figure 8. For most of the cases, the curve corresponding to the predicted rupture-time is indicating larger creep-rupture times. The difference between real and predicted values increases when both

temperature and the extrapolation time increases. In other words, the results in the present case show that it is possible to obtain smaller deviations in the predicted times if both the temperature and the extrapolation time are smaller. For instance, at the lowest temperature, the prediction time was correct up to 10000 hours.

As observed in Figure 9 the prediction in general results in higher rupture-times. However, this result must be examined carefully because the idea consists in using very short-time tests and extrapolating the results at much larger test times. The prediction certainly overestimates the life of the steel subjected to creep stresses. However, in all cases the material endured more time than the minimum requirements and that was accurately predicted. At this point, it is important to mention that slight variations in the magnitude of the constant C employed in the computation of P(σ) leads to large variations in the prediction time due to the logarithmic function involved. The actual experience suggests conducting experiments to assess its specific value in a future work.

Turbine manufacturers do not easily accept the idea of using results from short-times and extrapolating them to longer-times because of possible changes on steel microstructure. The results on microstructure after the creep-test consisted of 100% bainite with a homogeneous distribution of carbides. The additional increment in temperature during the creep tests can promote some extent of spheroidization of such carbides and this would be verified by a sudden decrease in hardness. However, when the actual hardness was measured and compared with that for short time tests, only a slight decrease was observed. Therefore, it is considered that the additional temperature increment in the range from 49 to 84°C did not negatively affect the microstructure.

4. Conclusion

The composition and heat treatment of 1.25Cr-1Mo-0.25V steels involving annealing, oil-quenching and

Table 4 - Real creep-rupture times.

Short-time rupture tests					Long-time rupture tests		
T, °C	σ, MPa	t_{real}, hr	LMP Eqn (4)	$t_{extrapol,hr}$	T, °C	σ, MPa	t_{real}, hr
599	200	178	19.38	3497	550	200	3521
617	175	149	19.78	10706	550	175	10426
634	150	226	20.18	32778	550	150	18533
626	**150**	**267**	**20.18**	**6208**	**575**	**150**	**5191**
645	**135**	**151**	**20.42**	**11910**	**575**	**135**	**7496**
656	**120**	**157**	**20.67**	**22851**	**575**	**120**	**13512**
652	120	253	20.67	4586	600	120	2840
677	100	120	20.99	10665	600	100	5016
684	90	121	21.15	16263	600	90	6869

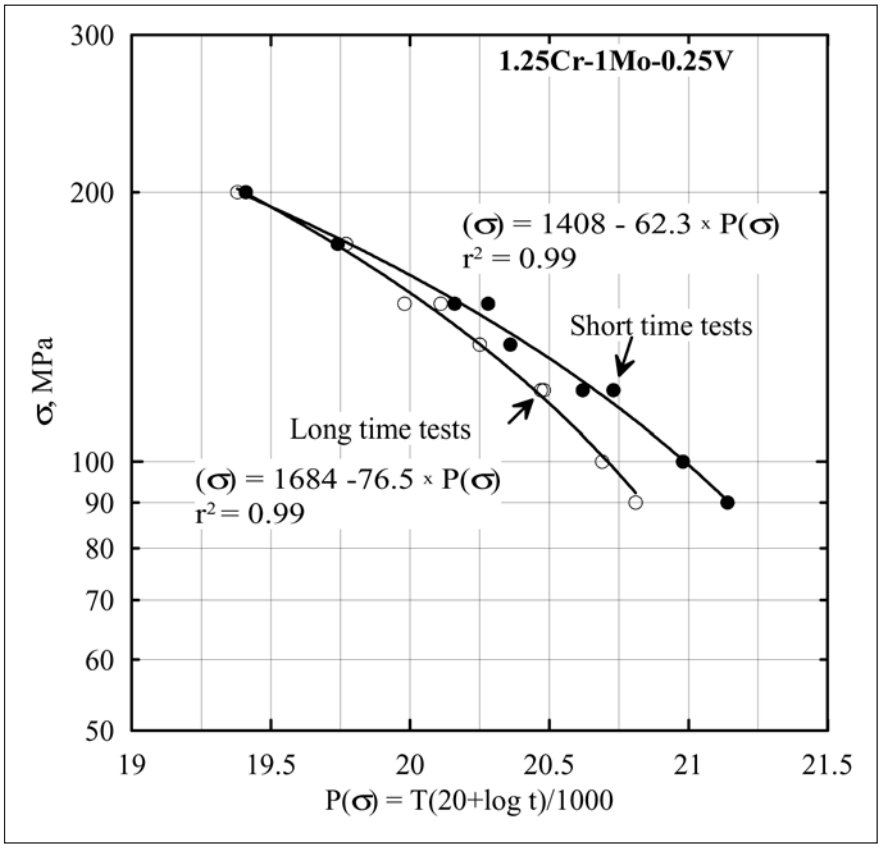

Figure 7 - Creep Master Curve.

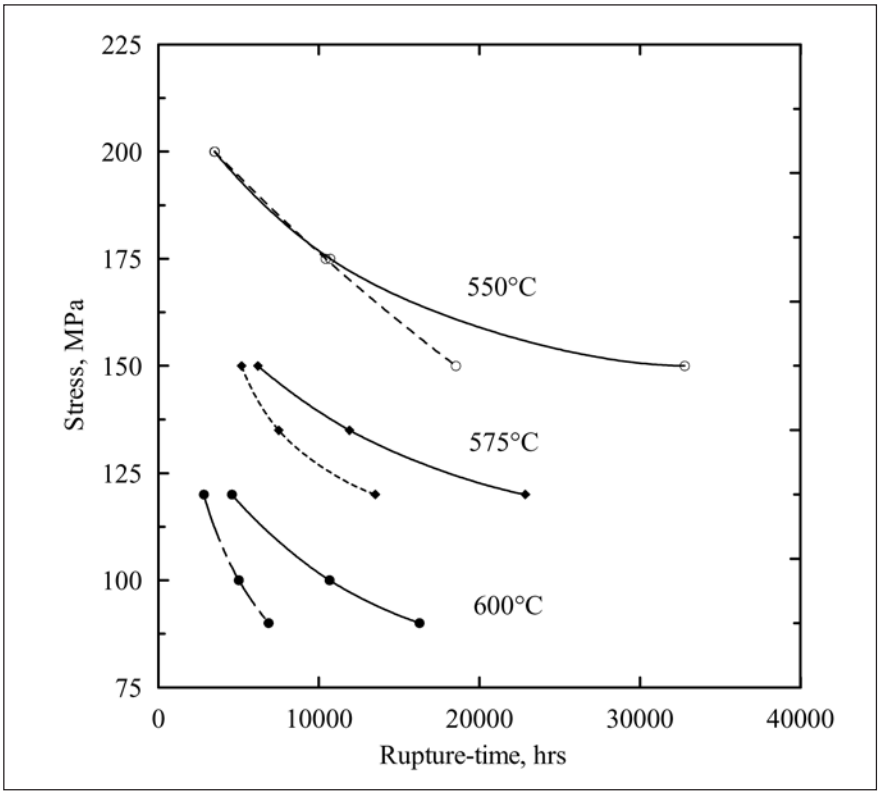

Figure 8 - Comparison of rupture strength using the real creep-rupture time (dotted lines)for "long-time" tests anda the predicted time(continuous lines) using data from "short-time" tests.

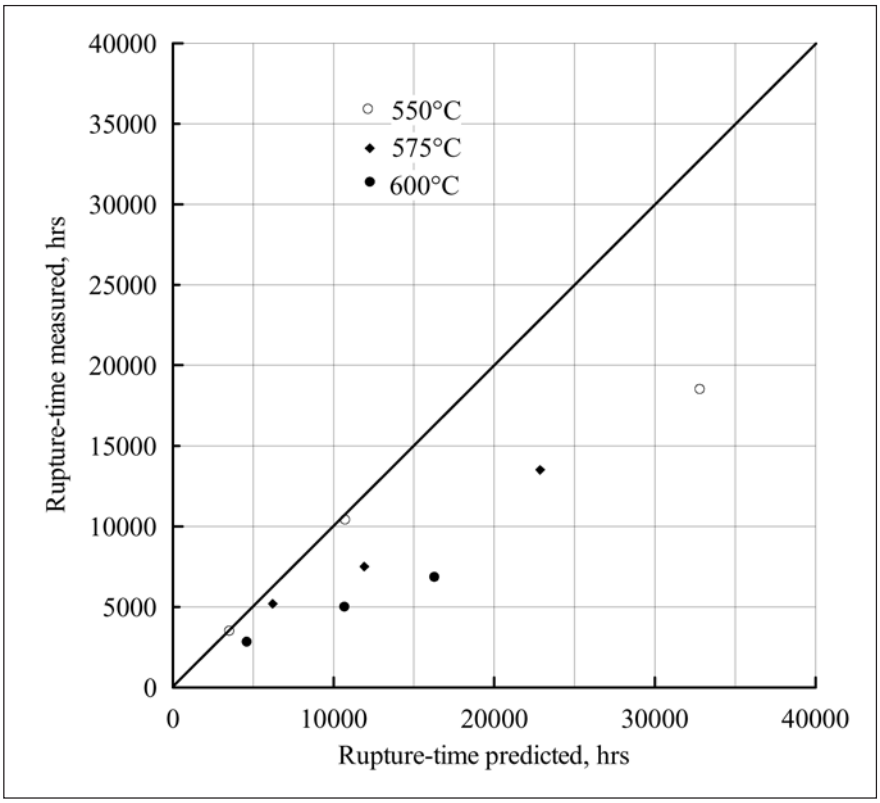

Figure 9 - Predicted versus measured creep-rupture times.

tempering was defined to yield high rupture-strength in the temperature range from 550-684°C. Application of the Larson Miller Parameter to extrapolate creep data from short-time tests (50 hrs) to longer times (1000-8000 hrs) was considered reliable for the conditions involved in the short-time creep tests conducted since no significant changes in the microstructure were identified for the increment in temperature from 49 to 84°C with respect to the nominal temperature. However, the predicted rupture-times are much higher than the real rupture-times and therefore unsatisfactory. Nevertheless, in spite of this finding, this procedure is considered extremely useful and can be used to take corrective actions during the manufacturing process to guarantee high creep-rupture strength in the final product.

5. Acknowledgements

Both authors acknowledge the permission from the management at NKS to report these results, in particular to H. Velasco, vice-president of quality assurance. Interesting discussions and suggestions with G. Gutierrez and E. Hurtado are greatly appreciated.

6. References

ASM, ***Metals Handbook***. 9th Edition, 1. 1978. p.643.
ASM. ***Metals Park Ohio***, USA. 1977.
ASTM standards (E139-96). ***Annual book***. 1996.
BUCHI, G.J.P., PAGE, J.H.R., SIDEY, M.P. ***JISI***. 291. 1965.
CIAS, W.W. Climax Molibdenum Co. USA: 1977.
DIETER, G. E. ***Mechanical metallurgy***. 2. ed. McGrawHill, 1976.
GROSSE-WOERDEMANN, J., DITTRICH, S. ***Metal progress***. 1982.
http://www.fe.doe.gov/international/mexiover.html.***An energy overview of México***. 2002.
KOBAYASHI, K., TSUCHIHARA, M., MURATA, M. ***JSW Technical Review***, n. 13, p. 30, 1977.
LARSON, F. R., MILLER, J. ***Trans ASME***, n. 74, p. 765, 1952.
Materials Characterization Laboratory (MCL). Scotia, New York, USA.
MASUYAMA, F. ***ISIJ Int.***, n. 41, p.612, 2001.
RIEDEL, H. ***Fracture at high temperatures***, SpringerVerlag-MRE, 1986.

Artigo recebido em 18/01/2005 e aprovado em 01/06/2005.